Highly Rotationally Excited CH 3 from Methane Photodissociation through Conical Intersection Pathway

ARTICLE *in* JOURNAL OF PHYSICAL CHEMISTRY LETTERS · JANUARY 2010

Impact Factor: 7.46 · DOI: 10.1021/jz900303e

4 AUTHORS, INCLUDING:

Kaijun Yuan
Dalian Institute of Chemical Physics
34 PUBLICATIONS **285** CITATIONS
SEE PROFILE

Xueming Yang
Dalian Institute of Chemical Physics
176 PUBLICATIONS **2,980** CITATIONS
SEE PROFILE

THE JOURNAL OF PHYSICAL CHEMISTRY Letters

pubs.acs.org/JPCL

Highly Rotationally Excited CH_3 from Methane Photodissociation through Conical Intersection Pathway

Yongwei Zhang, Kaijun Yuan,* Shengrui Yu, and Xueming Yang*

State key Laboratory of Molecular Reaction Dynamics, Dalian Institute of Chemical Physics, Chinese Academy of Sciences, 457 Zhongshan Road, Dalian, 116023, China

ABSTRACT Photodissociation of CH_4 has been studied using the high-resolution Rydberg tagging time-of-flight technique. The TOF spectra show an important single C−H bond fission channel with partially resolved sharp features. Careful simulations indicate that these sharp peaks are due to highly rotationally excited CH_3 products, which are likely produced through a conical intersection dissociation pathway between the excited and ground potential energy surfaces. The energy-dependent anisotropy parameter of the CH_3 product has also been determined at various photolysis wavelengths. The results of this work show that the conical intersection between the S_1 and S_0 surfaces plays an essential role in the photochemistry of CH_4.

SECTION Dynamics, Clusters, Excited States

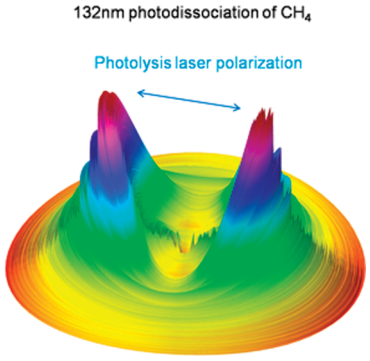

Photodissociation of methane (CH_4) plays an important role in both atmospheric and planetary chemistry. Methane is recognized as an important greenhouse gas and its photodissociation by solar radiation represents a major loss mechanism in the upper atmosphere. Furthermore, methane photodissociation is also believed to provide a synthetic route to the higher hydrocarbons which have been shown to be present in the atmosphere of the outer planets and their satellites, notably Titan.[1,2]

The electronic absorption spectrum of methane lies in the vacuum ultraviolet (VUV) region at wavelengths shorter than 140 nm. Extensive experimental and theoretical studies have been carried out in order to understand the photofragmentation of methane, particularly following excitation at the Lyman-α wavelength (121.6 nm).[3−10] Previous experimental studies indicated that the H_2 elimination channel accounted for nearly half of the total dissociation yield, with two other three-body forming channels responsible for the bulk of the remainder.[11] However, the first direct investigation of CH_4 photolysis using the H Rydberg atom photofragment translational spectroscopy method showed that simple C−H bond fission is also an important primary process, compared to the three-body channels.[7] Recently, Wang and Liu[5,6] reported a comprehensive Doppler-selected time-of-flight study of the H and D atom products from 121.6 nm photodissociation of CH_4 and all of its deuterated isotopomers. The study indicated that the three distinct pathways involved in C−H bond fission have different recoil anisotropy. In particular, two distinct dissociation pathways are elucidated for the two-fragment channel CH_3+H. Such behavior was rationalized by assuming that fragmentation occurs after radiationless transfer (internal conversion (IC) or intersystem crossing (ISC)) from the initially prepared excited singlet state. Recent ab initio calculations of Mebel et al.[12] confirmed that the main product channels, CH_2 ($\tilde{a}\ ^1A_1$) + H_2 and CH_3 ($\tilde{X}\ ^2A_2$) + H, do not correlate adiabatically with the excited state S_1 but rather with the ground state S_0. Thus, the photodissociation of methane is predominantly a nonadiabatic process with electronic transitions from the S_1 state to the S_0 state. As CH_3 ($\tilde{X}\ ^2A_2$) + H also correlates with the lowest triplet state T_1, spin−orbit couplings between the singlet and triplet states could provide an alternative mechanism, which produces CH_3 ($\tilde{X}\ ^2A_2$). Even though extensive studies for the photodissociation of methane have been performed, the nature of the nonadiabatic dynamics and the velocity-dependent recoil anisotropy remained unclear.

Conical intersections of potential energy surfaces are essential in the dynamics of excited electronic state dissociations and chemical reactions. The H_2O $\tilde{B}$ state photodissociation is one of the most well-known examples.[13,14] A remarkable feature for the conical intersection dissociation mechanism for H_2O is the extremely high rotational excitation of the OH product. The extreme rotational excitation is due to the conical intersection at the collinear geometry. Recently, several conical intersection seams between the ground state surface S_0 and the S_1 surface of methane have been suggested at planar geometries by Harrevelt.[15] However, the dynamical implications of the conical intersection for methane photochemistry have not yet been identified. This letter presents clear experimental evidence of highly rotationally excited CH_3 product from CH_4 photodissociation, which is

Received Date: November 23, 2009
Accepted Date: December 16, 2009
Published on Web Date: December 22, 2009

DOI: 10.1021/jz900303e | *J. Phys. Chem. Lett.* **2010**, *1*, 475–479

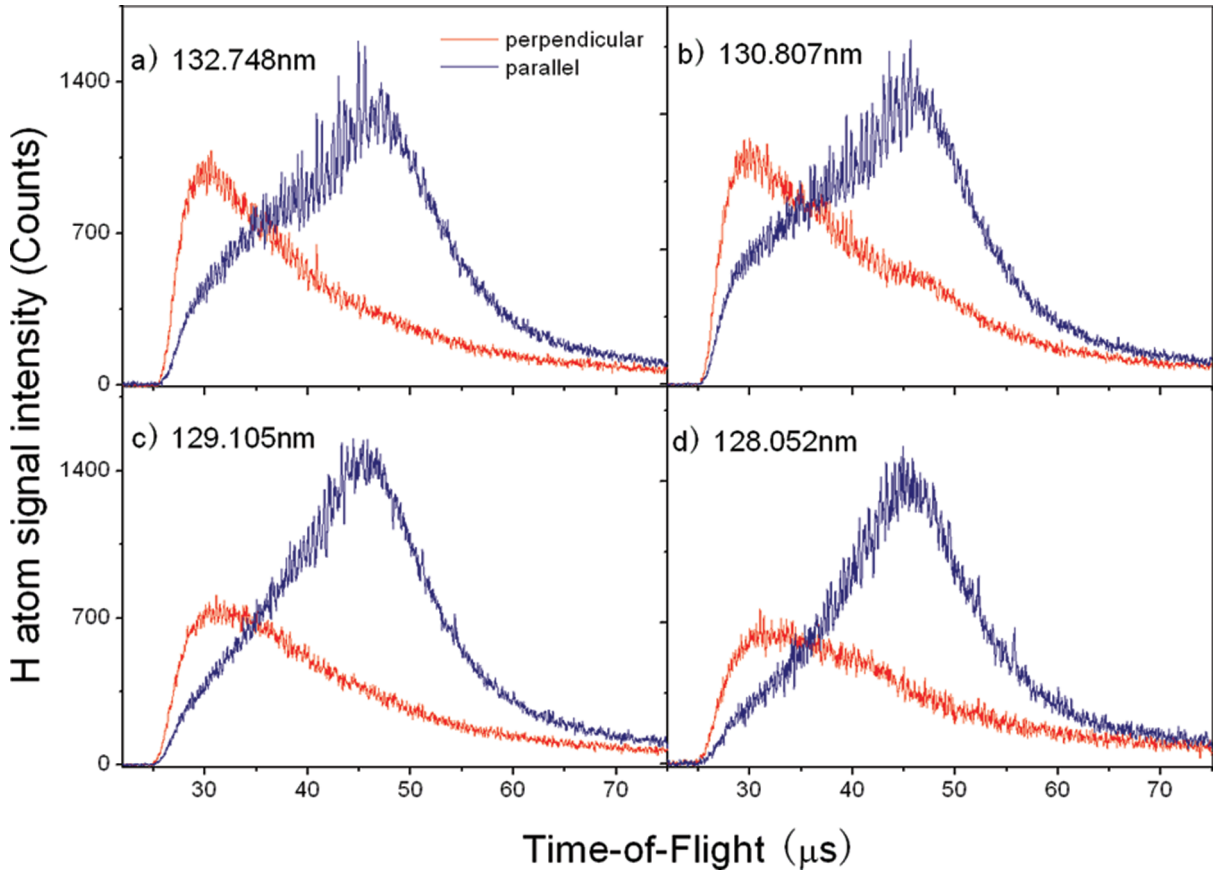

Figure 1. Time-of-flight spectra of the H atom product from the photodissociation of CH_4 at 132.748, 130.807, 129.105, and 128.052 nm with photolysis laser polarization parallel and perpendicular to the detection axis.

produced from the conical intersection pathway between the excited and ground potential energy surfaces.

We have recently developed a new method for investigating tunable VUV molecular photodissociation dynamics by using the H atom Rydberg tagging technique. This scheme has been applied to dissociation dynamics of CH_4 between 128 and 133 nm. Figure 1 shows the time-of-flight spectra of the H atom product from photodissociation of CH_4 at 132.748, 130.807, 129.105, and 128.052 nm using two different polarization schemes (parallel and perpendicular to the detection axis). TOF spectra of the H atom product at the magic angle polarization were also made to ensure that the intensity ratio of the TOF spectra obtained at parallel and perpendicular polarization is correct. Distinct differences in the spectral profiles for the two polarizations are noted, indicating significant anisotropy in the fragment angular distribution. In addition, many partially resolved sharp peaks have been seen in the parallel polarization direction. These sharp peaks gradually disappear as the photolysis energy increases. This is consistent with the previous studies at 121.6 nm.[4,5]

From the TOF spectra, the translational energy distributions can be obtained with a laboratory to center-of-mass transformation. Figure 2b shows the product translational energy distributions from CH_4 photodissociation at 132.748 nm. The threshold energy for all of possible H-atom elimination channels have been marked by downward pointing

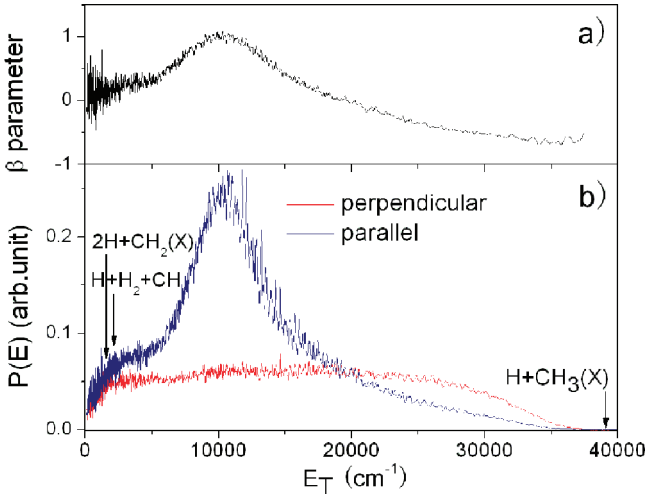

Figure 2. The translational energy distributions with photolysis laser polarization parallel and perpendicular to the detection axis (b), and anisotropy parameter β as a function of the total translational energy (a) for the photodissociation of CH_4 at 132.748 nm.

arrows. It is clear that the contributions of the three-body channels (slow H atom products) are much smaller than that at 121.6 nm photodissociation of CH_4. For $E_T \geq 2200$ cm^{-1}, the only chemical channel energetically accessible to the

DOI: 10.1021/jz900303e | J. Phys. Chem. Lett. 2010, 1, 475–479

H atom formation is the $CH_3(\tilde{X}\,^2A_2)$ + H pathway. Since the H-atom has no internal energy, the total translational energy distribution is also the internal energy distribution of the CH_3 ($\tilde{X}\,^2A_2$) product. Therefore, the partially resolved peaks in Figure 2b can only come from the rovibrationally excited CH_3 products.

Since translational energy distributions were measured for both parallel and perpendicular polarization, the anisotropy distribution $\beta(E)$ for the dissociation process can be determined from eq 1:[16]

$$f(E,\theta) = \varphi(E)(1+\beta(E)P_2(\cos\theta)) \quad (1)$$

where $\theta = 0°$ is for the parallel detection scheme, and $\theta = 90°$ is for the perpendicular detection scheme. Figure 2a displays the anisotropy parameter $\beta(E)$ as a function of the total translational energy. The β parameters start with a nearly isotropic angular distribution (the value is about 0) at low energy, rise gradually to a positive maximum followed by a drop, and cross over the $\beta = 0$ line to become negative with a value of -0.5 at high translational energies. This behavior is similar to that observed at 121.6 nm photolysis of CH_4,[5] suggesting the dynamics around 131 nm photodissociation is quite similar to that at 121.6 nm. The variation of the angular anisotropy parameter has been discussed by Liu et al.[5] and Cook et al.[4] Three district pathways with different anisotropy parameters have been used to simulate the translational spectra.[4,5] However, we found it is questionable to simulate the spectrum in that way at 132.748 nm photodissociation because the three-body H channels with anisotropy of $\beta \sim 0$ are very small. The CH_3+H channel with fixed β value cannot explain the observed spectrum in this experiment. Thus, another mechanism should be responsible for this peculiar rotationally dependent anisotropy parameter.

The most intriguing observation in the current experiment is the partially resolved sharp peaks in the translational spectra. These sharp peaks indicate that the partner CH_3 fragments are formed in a wide range of rovibronic states. The essential question that needs to be answered is whether CH_3 radical is highly rotationally excited or low rotationally excited. Ab initio calculations of Mebel et al.[12] found that the initial excitation of CH_4 around 130 nm is close to the $C_{3v}(A_1)$ geometry, and the geometry of the CH_3 fragment near the surface crossing region is very close to that of free CH_3 ($\tilde{X}\,^2A_2$). This means that the dissociation process favors populating only the out-of-plane bending vibrational levels of the CH_3 radical ($\nu_2 = 606\ cm^{-1}$). In order to understand the nature of the CH_3 internal excitation, we used the spectroscopic data of the CH_3 radical[17,18] to simulate the product translational energy distributions with two very different dissociation mechanisms. One is assuming that the $CH_3(\tilde{X}, \nu_2 = 0)$ products are highly rotationally excited with the peak of $N \sim 65$, while the other one is assuming that the CH_3 ($\tilde{X}, \nu_2 = 0$) products are low rotationally excited with its peak at small N. In both cases, limited in-plane rotation of CH_3 radical have been assumed by keeping the value of $K = 3$. These simple simulated results are shown in Figure 3a. It is obvious that the simulated translational distribution with high rotationally excited CH_3 products is more similar to the experimental result than the simulated translational energy distribution with low rotationally excited CH_3 products. The latter distribution is very different from the experimental result. If a considerable amount of the low rotationally excited CH_3 product is produced at various vibrational levels, a set of vibrational band heads should appear in the experiment translational energy distribution. A series of band heads has been observed in the product translational energy distribution in the photodissociation of H_2O via the $\tilde{C}$ state,[19] in which rotationally cold OH products at various vibrational levels are produced via a direct dissociation mechanism. In the current experiment, however, no such vibrational state band heads were observed in the product transitional energy distribution. These analyses strongly suggest that the CH_3 fragments are highly rotationally excited. Figure 3b also displays the possible assignments of the partially resolved sharp peaks. Most of peaks can be assigned as the rotational series $CH_3(\nu_2 = 0, N_0)$ and $CH_3(\nu_2 = 0, N_3)$. (Rotational states are marked as (ν, N_K), where ν is the quantum number of the ν_2 vibrational mode, and K is the rotational quantum number of the a-axis). The width of the individual peak is estimated to be 130 cm^{-1},

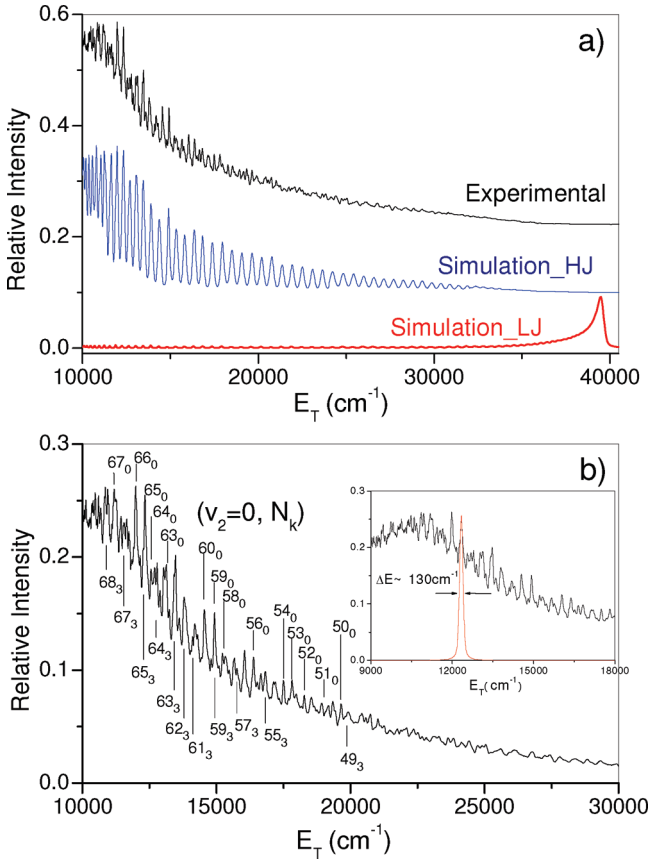

Figure 3. (a) Experimentally derived translational energy profile for photodissociation of CH_4 at 132.748 nm, together with two types of simulations: highly rotationally excited CH_3 mode (Simulation_HJ), and low rotationally excited CH_3 mode (Simulation_ LJ) with the value $\nu_2 = 0$, $K = 3$. (b) Possible assignments of the CH_3 rotational states (ν, N_k), where ν is the quantum number of the CH_3 ν_2 vibrational mode, and N_k is the quantum number of the CH_3 rotational state.

DOI: 10.1021/jz900303e | J. Phys. Chem. Lett. 2010, 1, 475–479

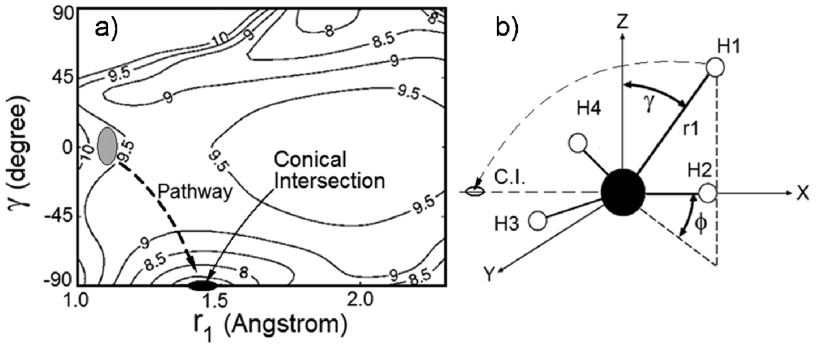

Figure 4. (a) The potential energy for the S_1 state as a function of r_1 and γ, at $\varphi = 0°$. (b) Coordinates used to illustrate the geometry changing, r_2, r_3, and r_4, are fixed at r_e, the range of the polar and azimuthal angles are $-90° \le \gamma \le 90°$ and $0° \le \varphi \le 180°$. The shaded area is the Franck−Condon excitation region. The dashed line with arrow is the conical dissociation pathway on the excited surface. This figure is modified from ref 15.

which is obviously much narrower than the width of an individual vibrational band head that is about 650 cm^{-1}. Therefore, the observed sharp peaks can be assigned to highly rotationally excited states of the CH_3 radical product. The CH_3 product is also probably somewhat vibrationally excited; this would cause rotational state congestions at high internal energy excitations of CH_3, which will make individual rotational states of CH_3 more difficult to be resolved in the translational energy distribution. Indeed, this is the case in the methane photodissociation. At higher photolysis energy, more vibrationally and rotationally (J and K quantum numbers) excited CH_3 radicals are produced, therefore, individual rotational structures are less resolvable in the translational energy distribution.

The key to understanding the dynamics producing the highly rotationally excited methyl radical and the energy dependent anisotropy is the remarkable shape of the potential energy surface of the S_1 state.[15] Figure 4 shows a contour plot of the potential energy surface with three C−H bond lengths fixed at equilibrium bond length $r_e = 1.086$ Å. The potential has two minima at planar geometries. The region around the deep minimum at $\gamma = -90°$ corresponds to the upper cone of a conical intersection of the S_0 and S_1 surfaces. When the trajectory approaches the conical intersection on the S_1 surface, it has a large probability to jump to the S_0 surface and reach CH_3 ($\tilde{X}\,^2A_2$) + H asymptote. Because the potential energy surface is repulsive in this region, the strong angular anisotropy makes the force almost perpendicular to the radial direction. The hydrogen atom moves toward the planar geometry, and gets a large amount of orbital angular momentum. At the same time, the CH_3 molecule rotates clockwise in order to compensate the change in angular momentum of the hydrogen atom. Thus, it is rationalized that the CH_3 products should be highly rotationally excited in this kind of dissociation mechanism. The other minimum at $\gamma = 90°$ is not a conical intersection. For this type of geometry, where two H atoms are quite close, it is more natural to dissociate into the $CH_2 + H_2$ channel.

The mechanism that produces highly rotationally excited CH_3 radical is very much similar to the cases of H_2O and NH_3. In both of these cases, very highly excited products, OH and NH_2, are produced via conical intersection pathways. Therefore, the results here provide a strong evidence that the conical intersection between the S_1 and S_0 surfaces plays an important role in the methane photodissociation. The variation of product anisotropy parameter is also rationalized through this conical intersection pathway. It is interesting that the anisotropy parameter for the high J products is higher than that for the low J products. This is because the generation of high J products requires the large angular forces during the dissociation. Similar rotational dependence of the anisotropy parameter for the radical product arising from a conical intersection pathway has also been observed in the H_2O[13] and NH_3[20] photodissociation. Future experiments in probing the angular distribution of the completely resolved rotational state of the CH_3 fragment will be particularly rewarding in unraveling the complete picture of this nonadiabatic dissociation process.

From the above study, we have presented experimental evidence that highly rotationally excited CH_3 products are generated from methane photodissociation. On the basis of previous theoretical results by Harrevelt, the highly rotationally excited CH_3 products are attributed to the conical intersection pathway between the S_1 and S_0 surface of methane. The rotational dependent anisotropy parameter is also consistent with this conjecture. Obviously, the conical intersection plays a very important role in the methane photochemistry, which has not been realized previously.

EXPERIMENTAL METHODS

In this work, photodissociation dynamics of CH_4 at wavelengths between 128 and 133 nm have been studied using the high H-atom Rydberg tagging time-of-flight (HRTOF) technique combined with a narrow-band, tunable VUV light source. Details of experimental setup used in this work have been described previously.[21,22] Briefly, the H-atom products in the photolysis region from the photodissociation of methane in the molecular beam are excited from the ground state to a high Rydberg state via a two-step excitation. The first excitation step was made by the 121.6 nm coherent light generated using difference four wave mixing (DFWM) of 212.5 and 845 nm in a Kr cell in which two photons of 212.5 nm are in resonance with a Kr 4p−5p[1/2,0] transition.[23] Following the VUV excitation, the H atom is then sequentially excited to a

DOI: 10.1021/jz900303e | J. Phys. Chem. Lett. 2010, 1, 475–479

high Rydberg state with $n \approx 60$ using a 365 nm radiation. The tunable VUV photolysis source (128−133 nm) was also generated using DFWM of the same 212.5 nm light for generating 121.6 nm and another tunable source λ_T (525−613 nm). The polarization of the photolysis source can be changed by rotating a polarization of the λ_T laser using a set of half waveplates. Since 121.6 nm also generates H atom signals, background subtraction was achieved by alternating the photolysis laser on and off. The neutral Rydberg-tagged H atoms then fly about 74 cm to reach a microchannel plate (MCP) detector, giving a TOF temporal resolution of about 0.3% or less. The detection axis, the molecular beam, and the photolysis laser beam are mutually perpendicular.

AUTHOR INFORMATION

Corresponding Author:

*To whom correspondence should be addressed. Email addresses: kjyuan@dicp.ac.cn (K.Y.); xmyang@dicp.ac.cn (X.Y.).

ACKNOWLEDGMENT This work is supported by the Chinese Academy of Sciences, the Ministry of Science and Technology, and the National Natural Science Foundation of China.

REFERENCES

(1) Wayne, R. P. *Chemistry of Atmospheres*: Clarendon: Oxford, U.K., 1991.
(2) Allen, M.; Pinto, J. P.; Yung, Y. L. Titan: Aerosol Photochemistry and Variations Related to the Sunspot Cycleq. *Astrophys. J.* **1980,** *242*, 125–128.
(3) Romanzin, C.; Gazeau, M. C.; Bénilan, Y.; Hébrard, E.; Jolly, A.; Raulin, F.; Boyé- Péronne, S.; Douin, S.; Gauyacq, D. Methane Photochemistry: A Brief Review in the Frame of a New Experimental Program of Titan's Atmosphere Simulations. *Adv. Space Res.* **2005,** *36*, 258–267.
(4) Cook, P. A.; Ashfold, M. N. R.; Lee, Y.-J.; Jung, K.-H.; Harich, S.; Yang, X. Vacuum Ultraviolet Photochemistry of Methane, Silane, and Germane. *Phys. Chem. Chem. Phys.* **2001,** *3*, 1848–1860.
(5) Wang, J.-H.; Liu, K. VUV Photochemistry of CH_4 and Isotopomers. I. Dynamics and Dissociation Pathway of the H/D-Atom Elimination Channel. *J. Chem. Phys.* **1998,** *109*, 7105–7112.
(6) Wang, J.-H.; Liu, K.; Min, Z.; Su, H.; Bersohn, R.; Preses, J.; Larese, J. Z. Vacuum Ultraviolet Photochemistry of CH_4 and Isotopomers. II. Product Channel Fields and Absorption Spectra. *J. Chem. Phys.* **2000,** *113*, 4146–4152.
(7) Mordaunt, D. H.; Lambert, I. R.; Morley, G. P.; Ashfold, M. N. R.; Dixon, R. N.; Schnieder, L.; Welge, K. H. Primary Product Channels in the Photodissociation of Methane at 121.6 nm. *J. Chem. Phys.* **1993,** *98*, 2054–2065.
(8) Schnieder, L.; Meier, W.; Welge, K. H.; Ashfold, M. N. R.; Western, C. M. Photodissociation Dynamics of H_2S at 121.6nm and a Determination of the Potential Energy Function of $SH(A^2\Sigma^+)$. *J. Chem. Phys.* **1990,** *92*, 7027–7037.
(9) Ashfold, M. N. R.; Mordaunt, D. H.; Wilson, S. H. S. *Advances in Photochemistry*; Wiley, New York, 1996; Vol. 21, p 217 and references therein.
(10) Heck, A. J. R.; Zare, R. N.; Chandler, D. W. Photofragment Imaging of Methane. *J. Chem. Phys.* **1996,** *104*, 4019–4030.
(11) Slanger, T. G.; Black, G. Photodissociative Channels at 121.6 Å for H_2O, NH_3, and CH_4. *J. Chem. Phys.* **1982,** *77*, 2432–2437.
(12) Mebel, A. M.; Lin, S.-H.; Chang, C.-H. Theoretical Study of Vibronic Spectra and Photodissociation Pathways of Methane. *J. Chem. Phys.* **1997,** *106*, 2612–2620.
(13) Harich, S. A.; Yang, X. F.; Huang, D. W.; Lin, J. J.; Yang, X. M.; Dixon, R. N. Photodissociation of H_2O at 121.6 nm: A State-to-State Dynamical Picture. *J. Chem. Phys.* **2000,** *113*, 10073–10090.
(14) Harich, S. A.; Yang, X. F.; Yang, X. M.; Dixon, R. N. Extremely Rotationally Excited OH from Water (HOD) Photodissociation through Conical Intersections. *Phys. Rev. Lett.* **2001,** *87*, 253201.
(15) Harrevelt, R. Photodissociation of Methane: Exploring Potential Energy Surfaces. *J. Chem. Phys.* **2006,** *125*, 124302.
(16) Zare, R. N. Photoejection Dynamics. *Mol. Photochem.* **1972,** *4*, 1–37.
(17) Yamada, C.; Hirota, E.; Kawaguchi, K. Diode Laser Study of the ν_2 Band of the Methyl Radical. *J. Chem. Phys.* **1981,** *75*, 5256–5264.
(18) Hermann, H. W.; Leone, S. R. Photofragment Infrared Emission Spectroscopy: Vibrational Progression and Potential Parameters of the $CH_3(\nu_2)$ Umbrella Mode. *J. Chem. Phys.* **1982,** *76*, 4759–4765.
(19) Yuan, K. J.; Cheng, Y.; Cheng, L. N.; Guo, Q.; Dai, D. X.; Yang, X. M.; Dixon, R. N. Dissociation Dynamics in H_2O: Competition Between Rotationally and Non-rotationally Mediated Pathways. *Proc. Natl. Acad. Sci. U.S.A.* **2008,** *105*, 19148.
(20) Ashfold, M. N. R.; Dixon, R. N.; Irving, S. J.; Koeppe, H. -M.; Meier, W.; Nightingale, J. R.; Schnieder, L.; Welge, K. H. Stereochemical and Angular Momentum Constraints in the Photodissociation of Ammonia. *Philos. Trans. R. Soc. London., Ser. A* **1990,** *332*, 375–386.
(21) Yuan, K. J.; Cheng, L. N.; Cheng, Y.; Guo, Q.; Dai, D. X.; Yang, X. M.; Tunable VUV Photochemistry Using Rydberg H-Atom Time-of-Flight Spectroscopy. *Rev. Sci. Instrum.* **2008,** *79*, 124101.
(22) Schnieder, L.; Seekamp-Rahn, K.; Wrede, E.; Welge, K. H. Experimental Determination of Quantum State Resolved Differential Cross Sections for the Hydrogen Exchange Reaction $H+D_2 \rightarrow HD+D$. *J. Chem. Phys.* **1997,** *107*, 6175–6195.
(23) Marangos, J. P.; Shen, N.; Ma, H.; Hutchinson, M. H. R.; Connerade, J. P. Broadly Tunable Vacuum-Ultraviolet Radiation Source Employing Resonant Enhanced Sum—Difference Frequency Mixing in Krypton. *J. Opt. Soc. Am. B* **1990,** *7*, 1254–1263.

DOI: 10.1021/jz900303e | *J. Phys. Chem. Lett.* **2010,** *1*, 475–479